Transient Analysis of Microwave Active Circuits Based on Time-Domain Characteristic Models

Qing-Xin Chu, Yuen-Pat Lau, and Fung-Yuel Chang, *Fellow, IEEE*

***Abstract*— A modular method is presented to speed up transient simulation of microwave active circuits which consist of linear components and active devices that are often nonlinear. Firstly, the linear components and active devices are individually characterized by time-domain characteristic models (TDCM's) and lumped equivalent circuits, respectively, to reduce the computer memory. Then, based on deconvolution, the TDCM's of linear components are synthesized from the terminal voltages and currents of step voltage excitation, which are simulated by the finite-difference time-domain (FDTD) method. Finally, transient analysis of a one-dimensional (1-D) discrete-time system is applied to obtain the terminal responses of the microwave active circuits, in which a larger sampled step is chosen to reduce the simulation time. This method is employed to two realistic circuits to validate its efficiency and accuracy. The results are in good agreement with the time-consuming direct FDTD simulation of entire circuits.**

***Index Terms*—FDTD method, microwave circuits, time-domain characteristic model, transient analysis.**

I. Introduction

MOST microwave active circuits are embedded with devices that are active and nonlinear. Since it is awkward to characterize the devices in frequency domain, time-domain analysis is well-suited for analyzing such system characteristics. The finite-difference time-domain (FDTD) method is the most suitable for this purpose because of its simple, robust, and flexible algorithm for numerical solution of Maxwell's equations [1]. Recently, the FDTD has been applied to analyze many microwave circuits such as oscillator [2], active antenna [3], [4], amplifier [5]–[7], and mixer [8]. In these applications, lumped elements are treated as subgrid models on an FDTD grid [2], [3], [8] or SPICE lumped circuits [4], [6], [7] are used to allow direct access to all SPICE models (via SPICE itself) for simulation of lumped circuits in FDTD calculations. However, computational requirements of FDTD are excessive due to the spacial–temporal discretization, especially for large circuits. Special care must be taken to avoid unstable oscillations and numerical instability when simulating nonlinear and active components, which causes inconvenience and increases computational time for FDTD analysis of microwave active circuits. For circuits including many discontinuities, responses with long time length must be calculated to obtain stable solutions. Besides, the spacial step of an FDTD mesh should be small for a highly accurate solution, which leads to a short time step by the Courant's stability criterion. It will take too much time when simulating the responses by a lengthy excitation.

Large microwave active circuits are built from many microwave components and lumped elements. One way to simulate a large circuit is to divide it into several small modules and then simulate them individually. The time-domain diakoptics method has been developed accordingly in the transmission-line matrix (TLM) [9], [10] and the FDTD method [11], [12]. All mutual interactions among modules are handled through a convolution interface. However, this approach may become quite cumbersome in the modeling of large complicated three-dimensional (3-D) circuits.

For most microwave circuits, what we are interested in are terminal voltages and currents at some ports, rather than distribution of electromagnetic fields in circuits. In other words, we are only interested in one-dimensional (1-D) variables at circuit ports, not 3-D variables showing field distribution in circuits. Based on this assumption, we present a modular computational method for transient simulation of terminal voltages and currents of microwave active circuits in this paper. In this method, a microwave active circuit is divided into linear components and nonlinear devices. Since the nonlinear devices in the microwave circuits are typically very small in size compared to a wavelength, they can be modeled by their lumped equivalent circuits with a very high degree of accuracy. The linear components are usually characterized with scattering parameters, which relate the incident and reflected waves at ports. However, for the FDTD computation of scattering parameters, the incident waves have to be calculated in advance on transmission lines or waveguides, which are the same as those that made up the ports of the network. For some components of microwave active circuits, which do not have ports with transmission lines or waveguides, it is difficult to calculate the incident waves. Besides, except the excitation port, all ports have to be terminated by matched loads when calculating the reflected waves. It means that nonreflected truncated boundaries should be imposed on the posts. Though various absorbing boundary conditions (ABC's) have been presented in the past, they cannot absorb all reflected waves. Therefore, ABC's are often set a distance away from ports to minimize unwanted effects. These treatments are complex and, thus, increase computational time.

A more suitable equivalent circuit for the linear components is the time-domain characteristic model (TDCM) [13], which relates the terminal voltages and currents at ports. One of the advantages in using the TDCM is that the TDCM can be synthesized from the terminal voltages and currents by waveform

Manuscript received June 6, 1997; revised May 11, 1998. This work was supported by Hong Kong UPGC under Grants CUHK RGC 294/94E.

The authors are with the Department of Electronic Engineering, Chinese University of Hong Kong, Shatin, N.T., Hong Kong.

Publisher Item Identifier S 0018-9480(98)05510-0.

relaxation iteration [14]–[16], where a linear component is driven by a step pulse voltage source at one port and loaded by resistors at other ports, which not only relaxes the restraint on loads at ports, but also includes the interaction between the component and loads. This procedure is briefly reviewed in Section II. Based on the models of linear components and nonlinear devices in hand, the terminal responses of the microwave active circuit are obtained by means of transient analysis of discrete-time systems. Besides the division of circuits to reduce the computer memory, another approach to reduce the computational time in this method is to enlarge the sampled step in simulation because there is no limitation of stability criterion as in FDTD simulation.

Two realistic examples are demonstrated in Section III to validate the method and illustrate the features. Good agreements are found when the simulated results are compared with direct FDTD simulations. Large reduction in computational time is observed. Finally, conclusions are drawn in Section IV.

II. Time-Domain Characteristic Model of a Linear Network

A linear component in the microwave active circuit can be considered as an N-port linear network. For the sake of conciseness, we shall focus the following discussion on the one- and two-port network. For a one-port network, the input impedance $Z_{\rm in}(\omega)$ is usually used as characteristic variable in the frequency domain, which is defined as

$$Z_{\rm in}(\omega) = \frac{V(\omega)}{I(\omega)} \tag{1}$$

where $V(\omega)$, $I(\omega)$ represent the terminal voltage and current in the frequency domain at the port, respectively. Transformed into the time domain, (1) becomes[1]

$$z_{\rm in}(t) = \frac{\{v(t)\}}{\{i(t)\}} \tag{2}$$

where $z_{\rm in}(t)$, the inverse Fourier transform of $Z_{\rm in}(\omega)$, is known as the transient input impedance, and $\{\cdots\}/\{\cdots\}$ denotes the deconvolution operator. For discrete-time systems, convolution operator is replaced by convolution summation as

$$v[n] = z_{\rm in}(t) * i(t) = \sum_{k=2}^{n} z_{\rm in}[n-k+1]i[k] + z_{\rm in}[n]i[1] \tag{3}$$

where $v[n] = v(n\Delta t)$, $i[n] = i(n\Delta t)$, $n = 1, 2, \cdots$, (Δt is the time step), and

$$z_{\rm in}[n] = \int_{(n-1)\Delta t}^{n\Delta t} z_{\rm in}(t)\, dt \tag{4}$$

which is known as the discrete transient input impedance. From (3), the deconvolution in the discrete-time system is formulated as

$$z_{\rm in}[n] = \frac{\{v[n]\}}{\{i[n]\}} = \frac{v[n] - \sum_{k=2}^{n} z_{\rm in}[n-k+1]i[k]}{i[1]}. \tag{5}$$

[1]Frequency- and time-domain functions are assigned by upper and lower case letters, respectively, such as $\{V(\omega), I(\omega)\}$ and $\{v(t), i(t)\}$.

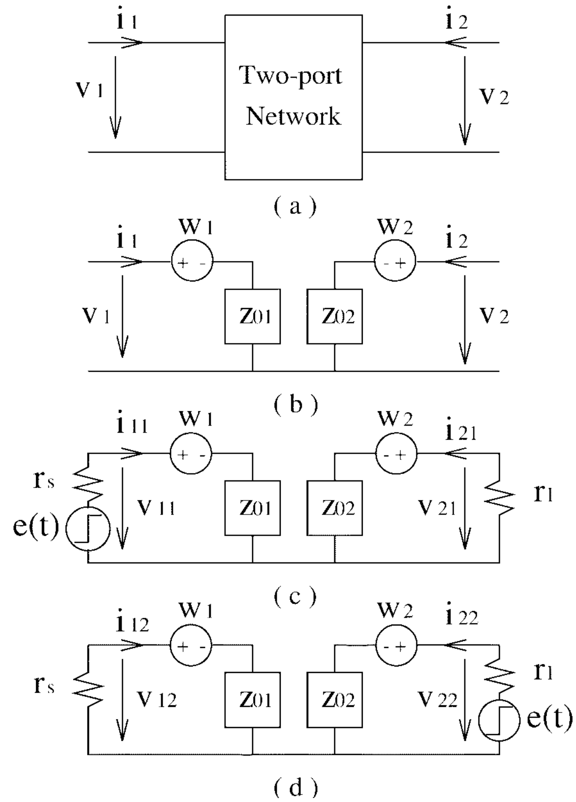

Fig. 1. (a) Linear two-port network. (b) TDCM. (c) Port 1 is derived by a voltage source and port 2 is terminated by a resistor. (d) Port 1 is terminated by a resistor and port 2 is drived by a voltage source.

The TDCM of a two-port network [see Fig. 1(a)] is shown in Fig. 1(b), which is described by the time-domain characteristic formulation

$$v_1(t) = z_{01}(t) * i_1(t) + w_1(t) \tag{6}$$

$$v_2(t) = z_{02}(t) * i_2(t) + w_2(t) \tag{7}$$

where

$$w_1(t) = h_1(t) * (v_2(t) + z_{02}(t) * i_2(t)) \tag{8}$$

$$w_2(t) = h_2(t) * (v_1(t) + z_{01}(t) * i_1(t)) \tag{9}$$

$\{v_1, i_1\}$, $\{v_2, i_2\}$ denote the terminal voltages and currents at ports 1 and 2, respectively. $\{z_{01}, h_1\}$, $\{z_{02}, h_2\}$ are known as the transient characteristic impedances and transfer functions of ports 1 and 2, respectively.

In order to apply the waveform relaxation algorithm, assume that a voltage source, giving step pulse excitation $e(t)$, and with an internal resistor r_s is imposed at port 1, and a resistor r_ℓ terminates port 2, as shown in Fig. 1(c). The terminal voltages at ports 1 and 2 are $v_{11}(t)$, $v_{21}(t)$, respectively. The terminal currents at ports 1 and 2 are

$$i_{11}(t) = \frac{e(t) - v_{11}(t)}{r_s} \tag{10}$$

$$i_{21}(t) = \frac{v_{21}(t)}{r_\ell}. \tag{11}$$

In the opposite direction [as shown in Fig. 1(d)], similar results can be obtained. Therefore, using the Gauss–Seidel iteration, we obtain the following iteration equations for the

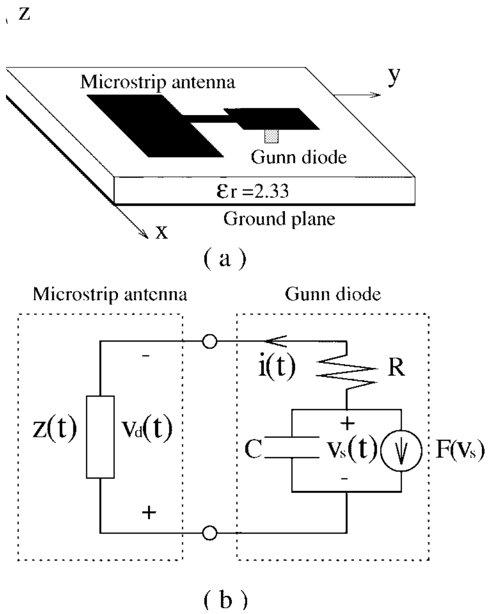

Fig. 2. (a) Layout of an active antenna. (b) Time-domain equivalent circuit.

transient characteristic impedances and transfer functions:

$$z_{01}^{(k)} = \frac{v_{11} - h_1^{(k-1)} * \hat{v}_{21}}{e - v_{11}} r_s \tag{12}$$

$$h_2^{(k)} = \frac{v_{21} + z_{02}^{(k-1)} * v_{21}/r_\ell}{v_{11} + z_{01}^{(k)}(e - v_{11})/r_\ell} \tag{13}$$

$$z_{02}^{(k)} = \frac{v_{22} - h_2^{(k)} * \hat{v}_{12}}{e - v_{22}} r_\ell \tag{14}$$

$$h_2^{(k)} = \frac{v_{12} + z_{01}^{(k)} * v_{12}/r_\ell}{v_{22} + z_{02}^{(k)}(e - v_{22})/r_s} \tag{15}$$

and

$$\hat{v}_{21} = v_{21} - z_{02}^{(k-1)} * v_{21}/r_\ell \tag{16}$$

$$\hat{v}_{12} = v_{12} - z_{01}^{(k)} * v_{12}/r_s \tag{17}$$

where k is iteration count. $h_1^{(0)} = z_{02}^{(0)} = 0$ is required for the zeroth iteration. For symmetric networks, $z_{01} = z_{02} = z_0$, $h_1 = h_2 = h$, thus, only (12) and (13) are needed.

III. Numerical Results

Two examples—an active antenna and a mixer—are considered to check the efficiency and accuracy of this method. FDTD analysis of the two circuits have been proved in [3] and [8].

A. Active Antenna

The active antenna consists of a microstrip antenna and a Gunn diode. Its layout and time-domain equivalent circuit are shown in Fig. 2. The active current source of the equivalent circuit for the Gunn diode is given by the polynomial

$$F(v_s) = -G_1 v_s + G_3 v_s^3 \tag{18}$$

where coefficient $G_1 = 0.0252\ \Omega^{-1}$, $G_3 = 0.0265\ \Omega^{-1}\ \mathrm{V}^{-2}$, capacitance $C = 0.2$ pF, and series resistance $R = 1.0\ \Omega$, as given in [3].

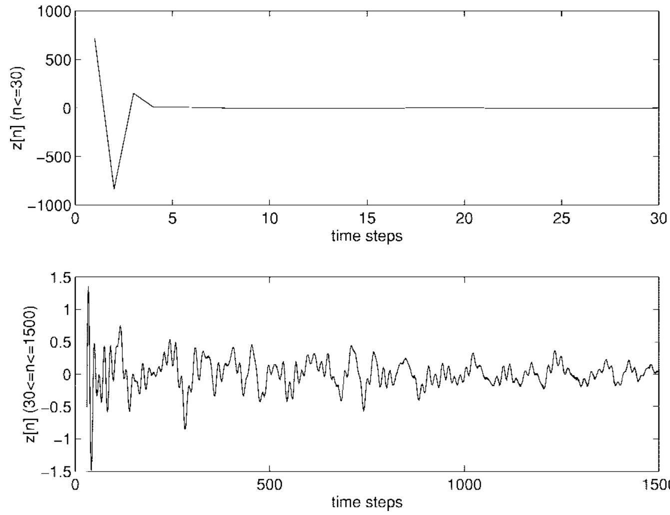

Fig. 3. Discrete transient impedance of microstrip antenna.

The microstrip antenna is equivalent to a transient input impedance $z(t)$ across the Gunn diode. In order to obtain the transient impedance, the Gunn diode is replaced by a resistive voltage source giving step pulse excitation. The terminal voltage $v(t)$ and current $i(t)$ are then calculated by the FDTD method. The process is called the FDTD characterization. The FDTD mesh space is $88\Delta x \times 138\Delta y \times 16\Delta z$, where $\Delta x = 0.5$ mm, $\Delta y = 0.5$ mm, and $\Delta z = 0.26$ mm. The waveforms are then substituted into (5). Fig. 3 shows the discrete transient impedance $z[n]$. Since $z[n]$ attenuates to zero rapidly, it is enough to calculate 1500 time steps, with a time step $\Delta t = 0.4$ ps. $z[n]$ is set to zero for $n > 1500$.

According to the equivalent circuit shown in Fig. 2(b), the voltage v_s and current i satisfy

$$C\frac{dv_s}{dt} + F(v_s) = -i \tag{19}$$

$$i = \frac{v_s + v_d}{R}. \tag{20}$$

Discretizing the above equations by time-average difference, we have

$$\left\{\frac{C}{\Delta t} + \frac{1}{2}\dot{F}(v_s[n])\right\} v_s[n+1] = \left\{\frac{C}{\Delta t} + \frac{1}{2}\dot{F}(v_s[n])\right\} v_s[n] - F(v_s[n]) - i\left[n + \frac{1}{2}\right] \tag{21}$$

and

$$i\left[n + \frac{1}{2}\right] = \frac{1}{2R}\left\{v_s[n+1] + v_s[n] + v_d[n+1] + v_d[n]\right\} \tag{22}$$

where $\dot{F}(v_s)$ denotes the derivative of $F(v_s)$ in terms of v_s.

Since the FDTD simulation of voltage and current is set off a half time step

$$v_d[n] = -\sum_{k=1}^{n} z[n-k+1]\, i\left[k - \frac{1}{2}\right]. \tag{23}$$

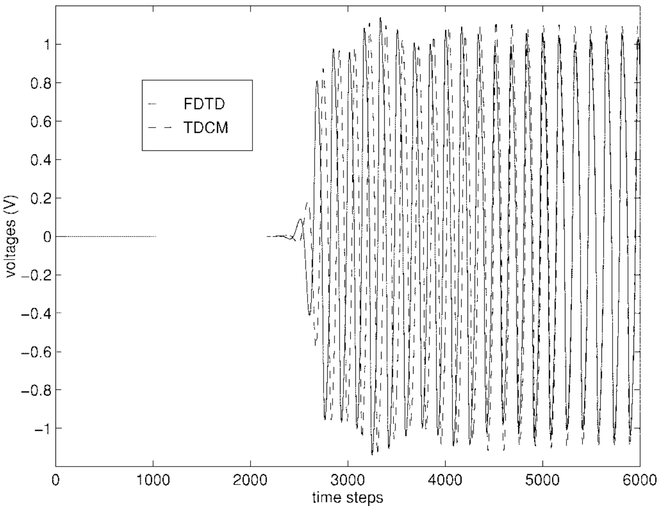

Fig. 4. Comparison of voltage across Gunn diode calculated based directly on the time-domain model and FDTD method.

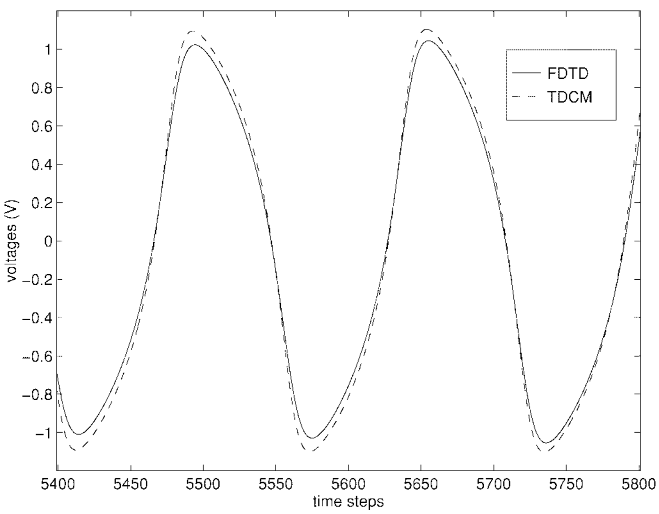

Fig. 5. Comparison of steady-state voltage across a Gunn diode calculated based directly on the time-domain model and FDTD method.

From (21) to (23), therefore, the difference equations for v_s and i are obtained as

$$v_s[n+1] = a_1 v_s[n] - a_2 F(v_s[n]) + a_2 v_z[n] \tag{24}$$

$$i\left[n+\frac{1}{2}\right] = \frac{1}{2R+z[1]}\,(v_s[n+1]+v_s[n]) - v_z[n] \tag{25}$$

where

$$a_1 = \frac{\dfrac{c}{\Delta t} + \dfrac{1}{2}\,\dot{F}(v_s[n]) - \dfrac{1}{2R+z[1]}}{\dfrac{c}{\Delta t} + \dfrac{1}{2}\,\dot{F}(v_s[n]) + \dfrac{1}{2R+z[1]}} \tag{26}$$

$$a_2 = \frac{1}{\dfrac{c}{\Delta t} + \dfrac{1}{2}\,\dot{F}(v_s[n]) + \dfrac{1}{2R+z[1]}} \tag{27}$$

$$v_z[n] = \sum_{k=1}^{n} \frac{z[n-k+2]+z[n-k+1]}{2R+z[1]}\, i\left[k-\frac{1}{2}\right] \tag{28}$$

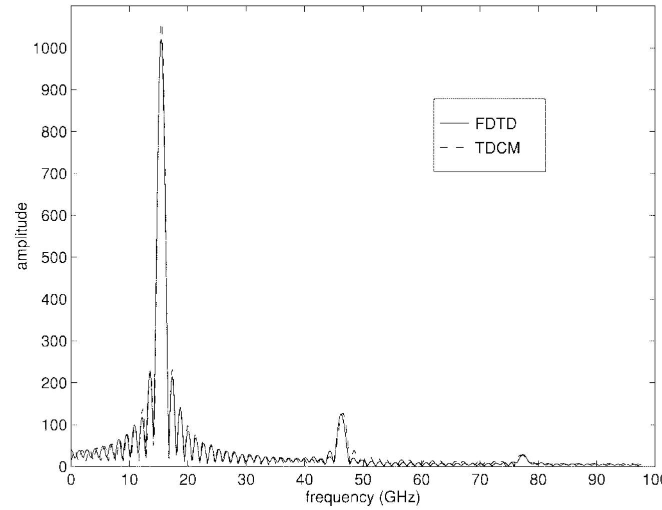

Fig. 6. Comparison of frequency spectrum of voltage across Gunn diode calculated based directly on the time-domain model and FDTD method.

TABLE I
COMPUTATIONAL TIME OF THE ACTIVE ANTENNA

Direct FDTD simulation:	10198 seconds
Simulation based on TDCM	
FDTD characterization:	2714 seconds
⋆ Circuit simulation:	6 seconds
Saved time:	7478 seconds

⋆ Transient function extraction has been included

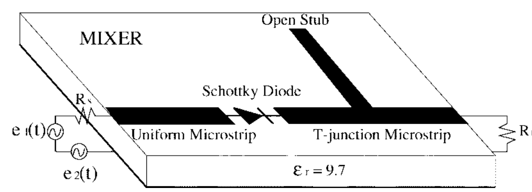

Fig. 7. Layout of an unbalanced mixer.

with the assumption that $i[(1/2)] = 0$, $v_s[1] = 10^{-20}$ V (noise). The voltage across the Gunn diode v_d is given by

$$v_d[n] = v_s[n] + R\frac{i\left[n+\dfrac{1}{2}\right] + i\left[n-\dfrac{1}{2}\right]}{2}. \tag{29}$$

Fig. 4 shows the calculated v_d based on the above equations (dashed line). The direct FDTD simulation is also carried out for comparison, which is also depicted in Fig. 4 as a solid line. It can be seen that both have good agreements, except some difference in transient state. Figs. 5 and 6 show both comparison of steady-state v_d and their frequency spectra, which are obtained by a discrete Fourier transform. Computational time based on the TDCM is about 4/15 compared with that of direct FDTD simulation, as shown in Table I.

B. Mixer

The drawing of an unbalanced mixer is shown in Fig. 7, in which a Schottky diode is connected between a uniform microstrip and a filtering microstrip stub in series. Two series-connected voltage sources are imposed at the input port, while the output port is terminated by a load resistor. In our simulation, the mixer system is divided into five modules, namely

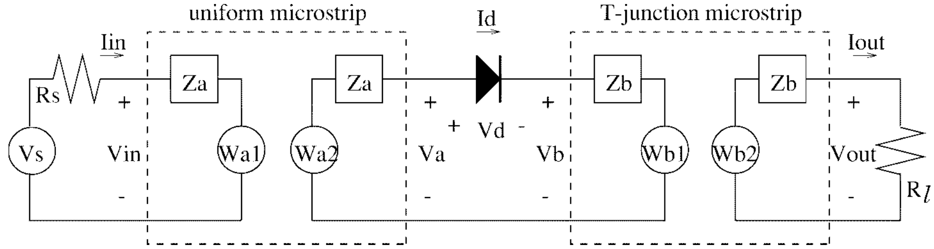

Fig. 8. Characteristic model of the mixer system.

two series-connected voltage sources, a uniform microstrip line, a Schottky diode, a T-junction with an open microstrip stub, and a load resistor. The voltage sources, diode, and load resistor are characterized by their lumped equivalent circuits, while the microstrip line and T-junction (both are symmetric) are characterized by the TDCM's. Fig. 8 shows the equivalent circuit of the mixer system. In order to extract the transient characteristic impedances and transfer functions of the uniform line and T-junction, a step excitation voltage source with 50-Ω internal resistor and a 50-Ω load resistor terminate the ports. The FDTD method is adopted to simulate the terminal voltages and currents. The FDTD mesh space is $26\Delta x \times 36\Delta y \times 10\Delta z$ for characterization of the uniform microstrip, while $166\Delta x \times 56\Delta y \times 10\Delta z$ for the T-junction, where $\Delta x = 0.1$ mm, $\Delta y = 0.1$ mm, and $\Delta z = 0.2$ mm. The time step $\Delta t = 0.2$ ps. $2000\Delta t$ is simulated for the uniform microstrip, and $8000\Delta t$ for the T-junction microstrip, so that the terminal voltages and currents reach the steady-state values. Then, the steady-state voltage and current values are expanded to make the entire waveforms having $80\,000\Delta t$, which is two cycle periods of output voltage of the mixer. These waveforms are then subsampled and each has 800 data points. Using waveform relaxation synthesis for symmetric circuits, we obtain the transient functions from the terminal responses. The discrete transient characteristic impedance $z_a[n]$ of the uniform microstrip line is shown in Fig. 9(a), together with the discrete transient transfer function $h_a[n]$, shown in Fig. 9(b). Fig. 10 shows the discrete transient characteristic impedance $z_b[n]$ and transfer function $h_b[n]$ of the T-junction microstrip.

Based on the equivalent circuit shown in Fig. 8, we derive four network equations, in the frequency domain

$$V_{\text{in}}(\omega) = H_a(\omega)(V_a(\omega) - Z_a(\omega)I_d(\omega)) + Z_a(\omega)I_{\text{in}}(\omega) \tag{30}$$

$$V_a(\omega) = H_a(\omega)(V_{\text{in}}(\omega) + Z_a(\omega)I_{\text{in}}(\omega)) - Z_a(\omega)I_d(\omega) \tag{31}$$

$$V_b(\omega) = H_b(\omega)(V_{\text{out}}(\omega) - Z_b(\omega)I_{\text{out}}(\omega)) + Z_b(\omega)I_d(\omega) \tag{32}$$

$$V_{\text{out}}(\omega) = H_b(\omega)(V_b(\omega) + Z_b(\omega)I_d(\omega)) - Z_b(\omega)I_{\text{out}}(\omega) \tag{33}$$

and two terminal conditions

$$I_{\text{in}}(\omega) = \frac{V_s(\omega) - V_{\text{in}}(\omega)}{R_s} \tag{34}$$

$$I_{\text{out}}(\omega) = \frac{V_{\text{out}}(\omega)}{R_\ell} \tag{35}$$

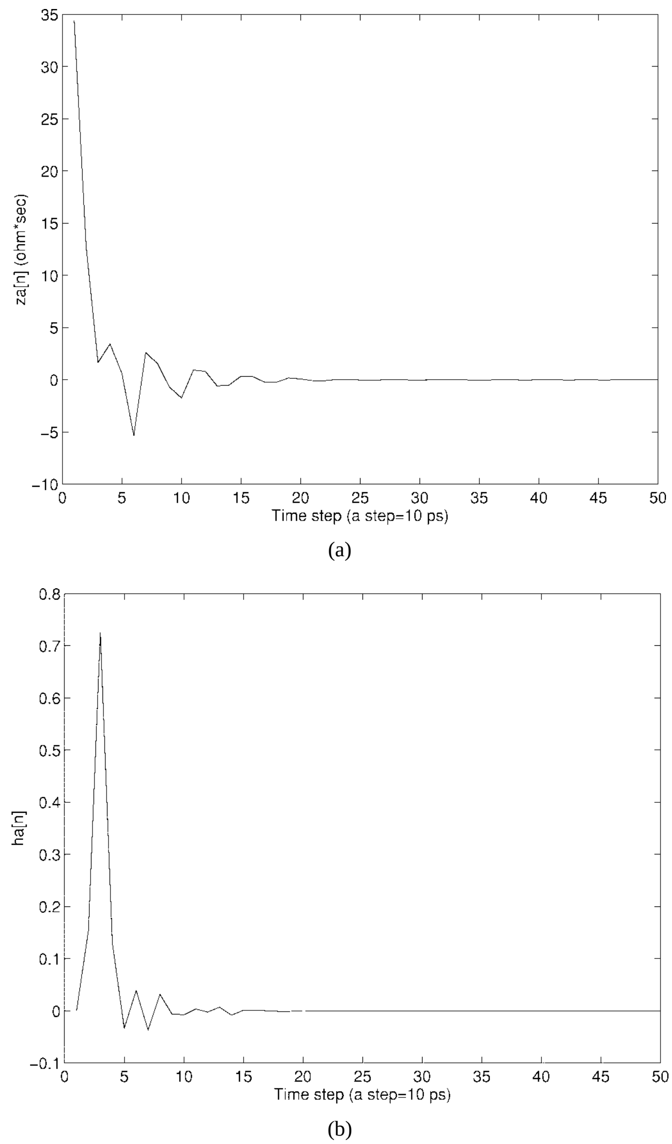

Fig. 9. Transient functions of the uniform microstrip.

where $R_s = R_\ell = 50\ \Omega$, and the voltage across the diode

$$V_d(\omega) = V_a(\omega) - V_b(\omega). \tag{36}$$

Eliminating all waveform variables except input voltage $V_{\text{in}}(\omega)$, output voltage $V_{\text{out}}(\omega)$, diode voltage $V_d(\omega)$, and diode current $I_d(\omega)$, and then transforming the equations into time domain, we have

$$v_d(t) - r_d(t) * i_d(t) = b_d(t) * v_s(t) \tag{37}$$

$$v_{\text{in}}(t) = b_s(t) * v_s(t) - r_{\text{in}}(t) * i_d(t) \tag{38}$$

$$v_{\text{out}}(t) = r_{\text{out}}(t) * i_d(t) \tag{39}$$

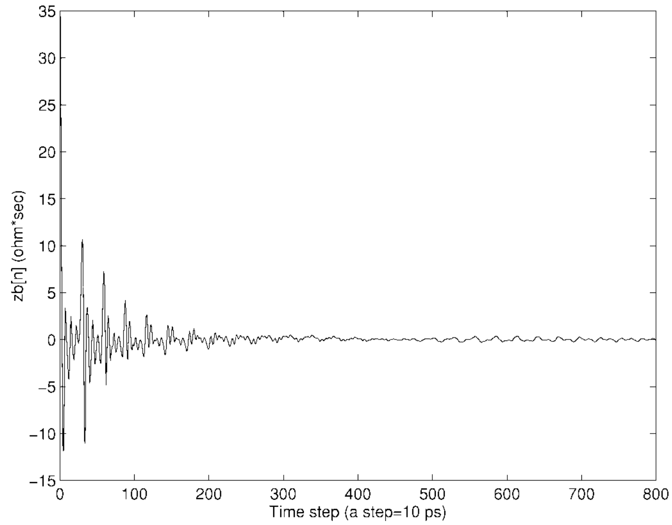

(a)

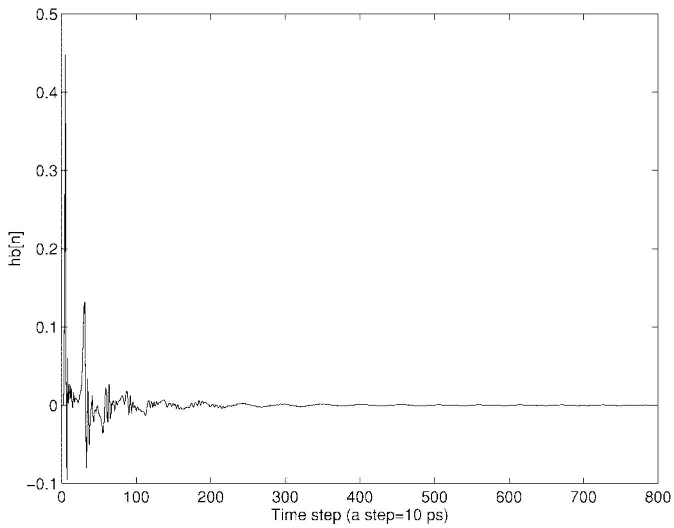

(b)

Fig. 10. Transient functions of the T-junction microstrip.

where $r_d(t)$, $r_{\rm in}(t)$, $r_{\rm out}(t)$, $b_d(t)$, and $b_s(t)$ are constructed by the transient functions and delta function $\delta(t)$. Circuit simulation is carried out by use of convolution summation on the discrete time version of (37)–(39). The source voltage and the *I–V* relation of the diode are given as [8]

$$v_s(t) = \sin(2\pi f_1 t) + \sin(2\pi f_2 t) \quad (40)$$

$$i_d(t) = I_0\left[\exp\left(\frac{qv_d(t)}{kT}\right) - 1\right] + C(v_d(t))\,\frac{dv_d(t)}{dt} \quad (41)$$

where $f_1 = 2$ GHz, $f_2 = 2.25$ GHz, $I_o = 2.48 \times 10^{-8}$ A, $kT/q = 25.9$ mV, and the junction capacitance of the diode is modeled by

$$\begin{aligned} C(v_d(t)) &= C(0)\left(1 - \frac{v_d(t)}{\Phi_0}\right)^{-m}, & v_d(t) < F_c\Phi_0 \\ &= \frac{C(0)}{F_2}\left(F_3 + \frac{mv_d(t)}{\Phi_0}\right), & v_d(t) \geq F_c\Phi_0 \end{aligned} \quad (42)$$

where $C(0) = 0.4$ pF, $\Phi_0 = 0.75$ V, $F_c = 1$, $F_2 = F_3 = 0.5$, and $m = 0.5$. Newton's method is employed to solve for the diode voltage from (37) and (42), since (37) is a nonlinear equation.

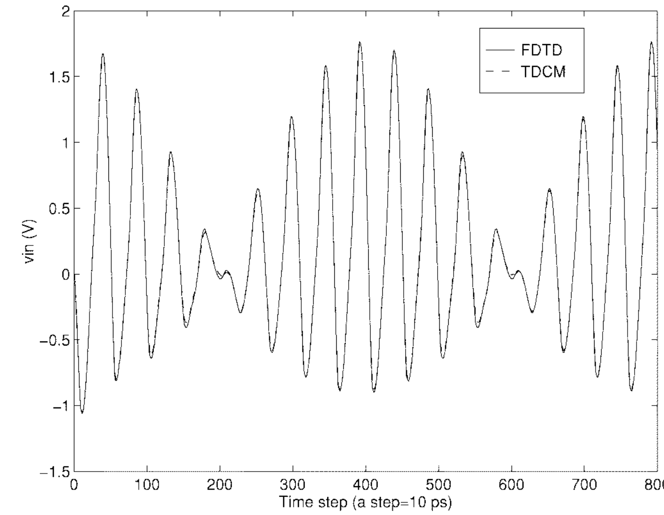

Fig. 11. Comparison of simulated input voltages.

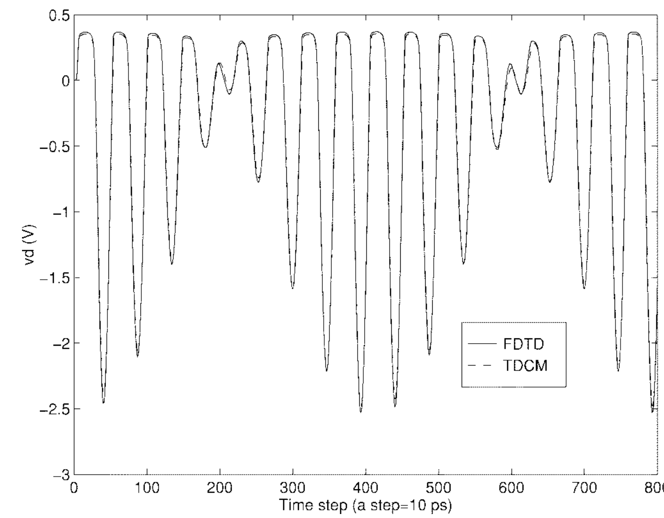

Fig. 12. Comparison of simulated diode voltages.

As described above, the time step is usually very small in FDTD simulation, since it is limited by the Courant's stability criterion. However, the criterion is unnecessary in the simulation based on TDCM's. Therefore, a large sampled step can be chosen, provided that each sampled waveform varies slowly. In other words, if the general shape of each sampled waveform is still maintained, the sampled step can be used. The sampled waveforms are used to calculate the sampled transient functions. These sampled transient functions are used to find the terminal voltages. As sampled data points are used for calculation, the simulation time is highly reduced. In this example, input, diode, and output voltages are simulated, each with 800 data points, as shown in Figs. 11–13 (dashed lines). Since the sampled step is $10\Delta t$, it means that the simulated period has 8000 ps.

Direct FDTD simulation for the mixer system is also carried out to validate the accuracy of the simulation based on the TDCM, in which the FDTD mesh space is $166\Delta x \times 73\Delta y \times$

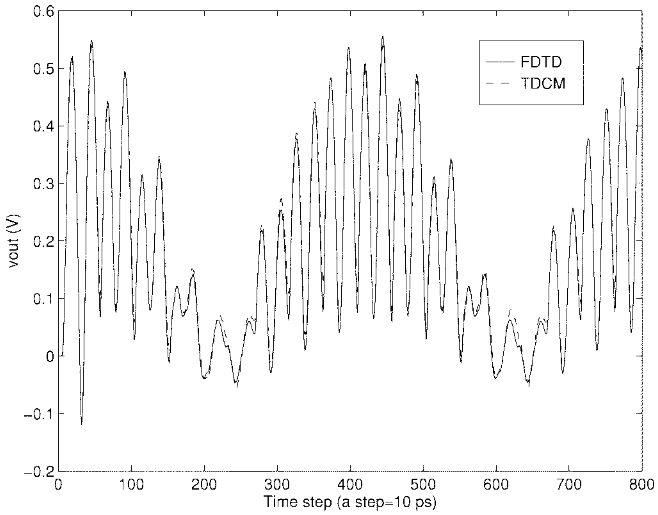

Fig. 13. Comparison of simulated output voltages.

TABLE II
COMPUTATIONAL TIME OF THE UNBALANCED MIXER

Direct FDTD simulation:	97214 seconds
Simulation based on TDCM	
uniform microstrip characterization:	151 seconds
T-junction microstrip characterization:	6294 seconds
⋆ Circuit simulation:	544 seconds
Saved time:	90225 seconds

⋆ Transient function extraction has been included

$10\Delta z$. Spacial steps are the same as that of the FDTD simulation of the uniform line and the T-junction, but the time step $\Delta t = 0.1$ ps, not 0.2 ps from Courant's stability criterion, to avoid divergence of a damped Newton–Raphson procedure to iteratively seek for the solution of electric field of the nonideal diode [8]. It means that 80 000 time steps must be carried out for 8000-ps simulation. Hence, the computational effort required by the simulation significantly increases when including nonlinear lumped elements.

The solid lines in Figs. 11–13 show input, diode, and output voltages simulated directly by FDTD. One can see that both results simulated directly by FDTD and based on the TDCM's have good agreement. Table II lists the comparison of both computational times. Computational time taken by the simulation based on TDCM is about 1/14 of that required by direct FDTD simulation.

IV. CONCLUSIONS

In this paper, we have presented a time-domain modular method to speed up transient analysis of microwave circuits. By dividing a large complex nonlinear circuit into linear components and nonlinear devices, then characterizing each individually in TDCM's or lumped equivalent circuits, computational memories are reduced. Since the limit imposed by Courant's stability criterion is broken, a large time step can be chosen for simulation. Thus, computation is speeded up significantly. When the circuit is modified, only a few segments need to be recalculated, the time-consuming repetitive computation of the entire circuit is avoided. Application to two realistic circuits has demonstrated the efficiency and accuracy of this method. We believe that this method may also become one candidate for the implementation of parallel computation in time-domain simulations. While a direct FDTD implementation including active devices will take into consideration all electromagnetic phenomena in the circuit (including mutual coupling, multimode competition, etc.), the proposed TDCM has significantly reduced the full-wave analysis capability by assuming a 1-D connection between the active device and segmentations of the passive circuit/antenna, which may fail to catch some of the wave phenomena in tightly integrated circuits where a full-wave analysis becomes important.

ACKNOWLEDGMENT

The authors are grateful to R. Sorrentino and L. Roselli for supplying the mixer details. They also thank the anonymous reviewers for their valuable comments.

REFERENCES

[1] K. S. Yee, "Numerical solution of initial boundary value problems involving Maxwell's equations in isotropic media," *IEEE Trans. Antennas Propagat.*, vol. AP-14, pp. 302–307, May 1966.
[2] B. Toland, B. Houshmand, and T. Itoh, "Modeling of nonlinear active regions with the FDTD method," *IEEE Microwave Guided Wave Lett.*, vol. 3, pp. 333–335, Sept. 1993.
[3] ——, "FDTD analysis of an active antenna," *IEEE Microwave Guided Wave Lett.*, vol. 3, pp. 423–425, Nov. 1993.
[4] V. A. Thomas, K. M. Ling, M. E. Jones, B. Toland, J. Liu, and T. Itoh, "FDTD analysis of an active antenna," *IEEE Microwave Guided Wave Lett.*, vol. 4, pp. 296–298, Sept. 1994.
[5] V. A. Thomas, M. E. Jones, M. Piket-May, A. Taflove, and E. Harrigan, "The use of SPICE lumped circuits as sub-grid models for FDTD analysis," *IEEE Microwave Guided Wave Lett.*, vol. 4, pp. 141–143, May 1994.
[6] C. N. Kuo, V. A. Thomas, S. T. Chew, B. Houshmand, and T. Itoh, "Small signal analysis of active circuits using FDTD algorithm," *IEEE Microwave Guided Wave Lett.*, vol. 5, pp. 216–218, July 1995.
[7] C. N. Kuo, R. B. Wu, B. Houshmand, and T. Itoh, "Modeling of microwave active devices using the FDTD analysis based on the voltage-source approach," *IEEE Microwave Guided Wave Lett.*, vol. 6, pp. 199–201, May 1996.
[8] P. Ciampolini, P. Mezzanotte, L. Roselli, D. Sereni, R. Sorrentino, and P. Torti, "Simulation of HF circuits with FDTD technique including nonideal lumped elements," in *IEEE MTT-S Int. Microwave Symp. Dig.*, Orlando, FL, May 14–19, 1995, pp. 361–364.
[9] P. B. Johns and K. Akhtarzad, "The use of time-domain diakoptics in time discrete models of fields," *Int. J. Numer. Methods Eng.*, vol. 17, pp. 1–14, 1981.
[10] W. J. R. Hoefer, "The discrete time-domain Green's function or Johns matrix—A new powerful concept in transmission line modeling (TLM)," *Int. J. Numer. Modeling*, vol. 2, pp. 215–225, 1989.
[11] T. W. Huang, B. Houshmand, and T. Itoh, "The FDTD Diakoptics method," in *IEEE MTT-S Int. Microwave Symp. Dig.*, Atlanta, GA, June 1993, pp. 1435–1438.
[12] ——, "Fast sequential FDTD Diakoptics method using the system identification technique," *IEEE Microwave Guided Wave Lett.*, vol. 3, pp. 378–401, Oct. 1993.
[13] F. Y. Chang, "Transient simulation of nonuniform coupled lossy transmission lines characterized with frequency-dependent parameters, Part I: Waveform relaxation analysis" *IEEE Trans. Circuit Syst. I*, vol. 39, pp. 585–603, Aug. 1992.
[14] ——, "Waveform relaxation synthesis of distributed-lumped network characteristic models," in *Proc. IEEE Int. Symp. Circuits Syst.*, vol. 5, London, U.K., 1994, pp. 29–32.
[15] Q. X. Chu and F. Y. Chang, "Waveform relaxation synthesis of time-domain characteristic model of two-port interconnects in high-speed circuits," in *Proc. IEEE Int. Symp. Circuits Syst.*, Hong Kong, June 1997, pp. 981–984.
[16] ——, "Waveform relaxation synthesis of time-domain characteristic model of microstrip from FDTD simulation," *IEEE Microwave Guided Wave Lett.*, vol. 7, pp. 161–164, June 1997.

[17] Q. X. Chu, F. Y. Chang, Y. P. Lau, and O. Wing, "Time-domain model synthesis of microstrip," *IEEE Microwave Guided Wave Lett.*, vol. 7, pp. 9–11, Jan. 1997.

Qing-Xin Chu was born on October 4, 1958, in Shaanxi, China. He received the B.S., M.S., and Ph.D degree in electronic engineering from Xidian University, Xi'an, China, in 1982, 1987, and 1994, respectively.

Since 1982, he has been with the Department of Microwave Telecommunication Engineering, Xidian University, as an Assistant Professor in 1983, Associate Professor in 1992, and Full Professor in 1997, respectively. He currently teaches graduate and undergraduate courses in electromagnetic theory, numerical methods in electromagnetics, and microwave circuits. From 1995 to 1997, he was with the Department of Electronic Engineering, Chinese University of Hong Kong, Hong Kong, as a Research Associate. His current research interests are in time-domain computational methods in electromagnetics, time-domain modeling of microwave circuits as well as high-speed circuits, and interaction of electromagnetic waves with material such as semiconductor chips.

Yuen-Pat Lau was born on August 15, 1972, in Fujian, China. He received the B.Eng. and M.Phil. degree in electronic engineering from the Chinese University of Hong Kong, Hong Kong, China, in 1995 and 1997, respectively.

His professional interests include time-domain circuit simulation of high-speed circuits and microwave circuits.

Fung-Yuel Chang (M'68–SM'88–F'93) received the B.S.E.E. degree with honors from the National Cheng Kung University, Taiwan, R.O.C., in 1959, the M.S.E.E. degree with honors from the National Chiao Tung University, Taiwan, R.O.C., in 1961, and the Eng.Sc.D. doctoral degree in electrical engineering from Columbia University, New York, NY, in 1968.

He joined the IBM Component Division, East Fishkill, NY, in 1968. His first job assignment at IBM led to the pioneering work on the method of characteristics for transient simulation of integrated circuits interconnected with multilayer dielectric coupled transmission lines. In his dual industrial and academic career, he has been an IBM Senior Engineering Manager, an Adjunct Full-Professor (1984–1992) of electrical engineering at Columbia University, a Visiting Professor of computer engineering at the University of California at Santa Cruz (1992–1993), and a Consultant for the Industrial Technology Research Institute (ITRI), Hsinchu, Taiwan, R.O.C. After becoming a Quarter-Century Club Member at IBM, he retired in 1993 and joined the faculty of the Department of Electronic Engineering, Chinese University of Hong Kong, Hong Kong, where he is currently a Visiting Professor. His research areas of interest include the computer simulation and experimental observation of wave propagation in very large-scale integration (VLSI) interconnects, computer-aided circuit analysis, dynamic device modeling, parallel computation, etc.

Dr. Chang has received many awards from industry, academic institutions, and professional societies, including the IBM Corporate Outstanding Innovation Award in recognition for his design and modeling of bipolar transistors implemented in three generations of IBM mainframe computers, the Columbia University School of Engineering and Applied Science Best Teaching Award (conferred to adjunct faculty member), and the IEEE Circuit and System Society Guillemin–Cauer Best Paper Award.